Bayesian/decision-feedback algorithm for blind adaptive equalization

K. Giridhar
John J. Shynk
Ronald A. Iltis
University of California
Center for Information Processing Research
Department of Electrical and Computer Engineering
Santa Barbara, California 93106

Abstract. A new blind equalization algorithm is presented that incorporates a Bayesian channel estimator and a decision-feedback (DF) adaptive filter. The Bayesian algorithm operates as a preprocessor on the received signal to provide an initial estimate of the channel coefficients. It is an approximate maximum *a posteriori* (MAP) sequence estimator that generates reliable estimates of the transmitted symbols. These decisions are then filtered by an adaptive decision-feedback algorithm to further reduce the intersymbol interference. The new algorithm is more robust to catastrophic error propagation than the standard decision-feedback equalizer (DFE), with only a modest increase in the computational complexity.

Subject terms: adaptive signal processing; blind equalization; sequence estimation; Bayesian equalizer; decision-feedback equalization.

Optical Engineering 31(6), 1211-1223 (June 1992).

1 Introduction

Blind equalization algorithms attempt to identify a transmitted symbol sequence in the presence of intersymbol interference (ISI) without resorting to a training sequence. Existing blind equalization algorithms can generally be classified into two categories: (a) those based on Bussgang techniques and (b) those based on high-order statistics.[1] The Bussgang-type algorithms are derived by minimizing a nonconvex performance function using gradient-descent techniques. As shown in Fig. 1, the received signal is passed through a linear transversal filter, yielding an estimate $y(k)$ of the transmitted sequence. This linear estimate is then processed by a zero-memory nonlinearity, $g[y(k)]$, to generate the "desired response," $\hat{d}(k-\Delta)$, which is used in the error signal of a gradient-descent algorithm. Several types of nonlinearities have been studied by many authors,[2-8] leading to a family of Bussgang-type algorithms. Although simple to implement, these algorithms exhibit slow convergence and may converge to undesirable local minima.[9] A comparative performance study of several Bussgang-type algorithms is presented in Ref. 10, illustrating some of their transient and steady-state convergence properties. Blind adaptive algorithms based on high-order statistics use cumulants of the received signal to directly extract phase information about the channel.[11] These algorithms have a faster initial convergence rate than the Bussgang-type algorithms, but they usually have a greater computational complexity.

In contrast to both of these approaches, blind equalization algorithms that approximate the optimum maximum *a posteriori* (MAP) sequence estimator[12] for *unknown* channels were recently introduced.[13-15] These algorithms achieve blind start-up and have rapid convergence (usually within 200 iterations), even for channels with deep spectral nulls. Joint channel estimation and data recovery algorithms based on the maximum-likelihood principle have also been proposed.[16-18] However, because the sequence estimator in these algorithms is a Viterbi decoder, the decisions have a decoding delay that could be quite large. The MAP estimator, on the other hand, produces delay-free decisions that can be exploited to reduce the complexity of the algorithm, as discussed in Secs. 2 and 3.

The exact MAP sequence estimator requires a separate channel estimate for each possible symbol sequence, and therefore its computational complexity grows exponentially with time. To overcome this complexity problem, a suboptimum Bayesian recursion[14] was developed for the MAP sequence probabilities by maintaining separate channel estimates for only M^{N_b+1} *subsequences*, where M is the symbol alphabet size and N_b+1 is the (estimated) length of the channel impulse response. The resulting algorithm can be implemented using a bank of Kalman filters in which each filter maintains a channel estimate conditioned on one of the M^{N_b+1} subsequences. Note that the complexity of this Bayesian method grows exponentially with the number of symbols, whereas the complexity of Bussgang-type and cumulant-based algorithms is essentially independent of M. To reduce the complexity for large signal constellations, reduced-state sequence estimation[19] (RSSE) was employed. In RSSE, the M^{N_b+1} subsequences are grouped into a coarser partition of $J \leq M^{N_b+1}$ subsets, and the number of Kalman channel estimators is correspondingly reduced. Finally, as

Paper SP-007 received July 31, 1991; revised manuscript received March 6, 1992; accepted for publication March 9, 1992.

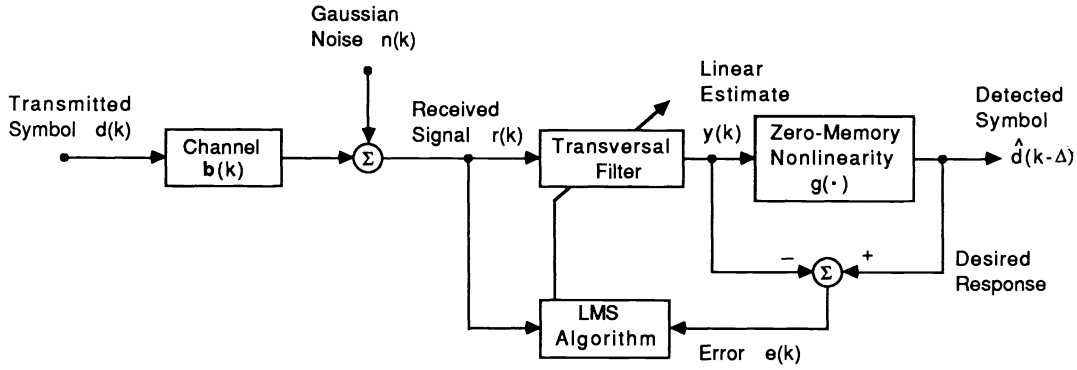

Fig. 1 Bussgang configuration for blind equalization.

a further simplification, the Kalman estimators were replaced by least-mean-square (LMS) adaptive filters, thus avoiding updates of covariance-type matrices.

In this paper, we present a modified Bayesian algorithm that incorporates *decision feedback* to further reduce the computational complexity. For channels with a long impulse response, the equalization process can be divided between the parallel LMS Bayesian filter bank and a single decision-feedback (DF) filter. The filter bank first removes the ISI due to the dominant channel coefficients, and the feedback filter compensates for the remaining ISI caused by the tail of the channel impulse response. Since a channel typically has only a few dominant coefficients, the complexity of this combined Bayesian/DF algorithm (BDFA) is considerably less than that of the original Bayesian algorithm in Ref. 14.

By varying how the coefficient estimates are shared between the Bayesian filter bank and the DF filter, the operation of the BDFA can be varied between that of a decision-feedback equalizer (DFE) and that of the full Bayesian algorithm. Thus, there is a trade-off between the computational complexity of the algorithm and its initial error-rate performance. In particular, the size of the Bayesian filter bank should be sufficiently large to prevent any catastrophic error propagation in the DF filter. The DF algorithm operates smoothly with the Bayesian symbol detection algorithm and it outperforms RSSE, which was originally developed to reduce the complexity of the Viterbi algorithm (VA) for maximum-likelihood sequence estimation[19] (MLSE).

The paper is organized as follows. The MAP estimation problem is briefly discussed in Sec. 2, and the LMS Bayesian equalization algorithm is reviewed using the notation of Ref. 14. The motivation for incorporating decision feedback is also given, and its advantages over RSSE are discussed. The new Bayesian/decision-feedback algorithm is then presented in Sec. 3. Computer simulations are given in Sec. 4, and the properties of the BDFA are discussed in Sec. 5. Conclusions are outlined in Sec. 6.

2 MAP Estimation Algorithm

In the original development of the suboptimal Bayesian channel estimator, the following discrete-time channel model was assumed[14]:

$$r(k)=\sum_{m=0}^{N_b} b_m(k)d(k-m)+n(k) \ , \tag{1}$$

where $r(k)$ is the output of a matched and prewhitening filter at time k, $d(k)$ is the most recent transmitted symbol, and $\{b_m(k)\}$ are the time-varying "channel" coefficients. These coefficients are obtained as the convolution between the actual channel impulse response, the matched filter impulse response, and that of a prewhitening filter, which is included to ensure that the additive noise $n(k)$ is an uncorrelated process. This noise is assumed to be a complex Gaussian sequence with zero mean and variance σ_n^2. Perfect synchronization is implicitly assumed in the above model.

Define the following channel coefficient (column) vector:

$$\mathbf{b}(k)=[b_0(k),b_1(k),\ldots,b_{N_b}(k)]^T \ , \tag{2}$$

which, in general, can be complex-valued. Of the M^{N_b+1} possible subsequences comprising the data symbols associated with Eq. (2), define the i'th subsequence as

$$d_i^{k,N_b}=\{d_i(k),d_i(k-1),\ldots,d_i(k-N_b)\} \ , \tag{3}$$

which can be written in (row) vector notation as

$$\mathbf{h}_i(k)=[d_i(k),d_i(k-1),\ldots,d_i(k-N_b)] \ . \tag{4}$$

Finally, define the *cumulative* measurement sequence r^k, which represents the matched filter output collected up to time k, as follows:

$$r^k=\{r(k),r(k-1),\ldots,r(0)\} \ . \tag{5}$$

In the suboptimum MAP sequence estimator, the probability density function of the channel coefficient vector is modeled as a complex Gaussian vector when *conditioned* on the cumulative observations r^{k-1} and the i'th data subsequence d_i^{k,N_b}, i.e.,

$$p[\mathbf{b}(k)|d_i^{k,N_b},r^{k-1}]=\mathcal{N}[\mathbf{b}(k);\hat{\mathbf{b}}_i(k-1),\ \mathbf{I}] \ , \tag{6}$$

where $\mathcal{N}(\mathbf{x};\mathbf{m},\mathbf{P})$ is a circular multivariate Gaussian density with mean vector $\mathbf{m}$ and covariance matrix $\mathbf{P}$. The true

density of $\mathbf{b}(k)$ conditioned on a given subsequence, d_i^{k,N_b}, is actually a weighted sum of Gaussian densities with the weights given in terms of the MAP sequence probabilities $p(d_j^{k-1,N_b}|r^{k-1})$ at time $k-1$. However, the density is approximated as being unimodal in Eq. (6) with mean denoted by $\hat{\mathbf{b}}_i(k-1)$, assuming that one of the MAP sequence probabilities is close to 1 and the others are nearly 0. This approximation yields a blind equalizer based on a parallel bank of adaptive filters. By assuming that the covariance matrix is given by the identity matrix $\mathbf{I}$, the weight updates for the adaptive filters reduce to simple gradient-descent algorithms.

The MAP estimate of subsequence d_i^{k,N_b} is

$$p(d_i^{k,N_b}|r^k)=\frac{1}{c}p[r(k)|d_i^{k,N_b},r^{k-1}] \times \sum_{\{j:d_j^{k-1,N_b}\in d_i^{k,N_b}\}} p(d_j^{k-1,N_b}|r^{k-1}) \ , \tag{7}$$

where c is a normalization constant. In the above expression, observe that subsequence $d_j^{k-1,N_b} \in d_i^{k,N_b}$ implies that the first N_b symbols in subsequence d_j^{k-1,N_b} equal the last N_b symbols in d_i^{k,N_b}. For example, with $N_b+1=4$ and assuming binary phase-shift keying (BPSK) (± 1), if $d_j^{k-1,N_b}=\{-1,1,1,-1\}$ and $d_i^{k,N_b}=\{1,-1,1,1\}$, we have $d_j^{k-1,N_b}\in d_i^{k,N_b}$. Under the approximation of Eq. (6), the likelihood $p[r(k)|d_i^{k,N_b},r^{k-1}]$ is a Gaussian density, as follows:

$$p[r(k)|d_i^{k,N_b},r^{k-1}]=\mathcal{N}[r(k);\hat{r}_i(k),\sigma_i^2(k)] \ . \tag{8}$$

The mean $\hat{r}_i(k)$ corresponding to the symbol estimate based on the i'th subsequence, is computed as

$$\hat{r}_i(k)=\sum_{m=0}^{N_b}\hat{b}_{i,m}(k-1)d_i(k-m) \ , \tag{9}$$

and the covariance is

$$\sigma_i^2(k)=\mathbf{h}_i(k)\mathbf{h}_i^H(k)+\sigma_n^2 \ , \tag{10}$$

where the superscript H denotes complex conjugate transpose. This covariance has a simple form because of the identity matrix in Eq. (6), and we further simplify it as $\sigma_i^2(k)=\sigma^2$, $\forall i$ and $\forall k$. The update for the *conditional* coefficient measurement, $\hat{\mathbf{b}}_i^c(k)$, is then given by

$$\hat{\mathbf{b}}_i^c(k)=\hat{\mathbf{b}}_i(k-1)+\mu(k)\mathbf{h}_i^H(k)[r(k)-\hat{r}_i(k)] \ , \tag{11}$$

where $\mu(k)$ is an adjustable gain factor that incorporates σ^2.

To complete the recursion, the "unconditional" channel estimate, $\hat{\mathbf{b}}_i(k)$, must be derived. It is shown in Ref. 14 that this can be expressed as a weighted linear combination of the conditional estimates $\hat{\mathbf{b}}_j^c(k)$, with weights that are the appropriately scaled MAP sequence probabilities, i.e.,

$$\hat{\mathbf{b}}_i(k)=\sum_{\{j:d_j^{k,N_b}\in d_i^{k+1,N_b}\}}\alpha_j\hat{\mathbf{b}}_j^c(k) \ , \tag{12}$$

where

$$\alpha_j=\frac{p(d_j^{k,N_b}|r^k)}{\sum_{\{m:d_m^{k,N_b}\in d_i^{k+1,N_b}\}}p(d_m^{k,N_b}|r^k)} \tag{13}$$

This result is derived from the fact that $p[\mathbf{b}(k+1)|d_i^{k+1,N_b},r^k]$ is a Gaussian sum with coefficients α_j even when $p[\mathbf{b}(k)|d_i^{k,N_b},r^{k-1}]$ in Eq. (6) is approximated as a unimodal Gaussian density. In effect, the conditioning on symbol $d_j(k-N_b)$ is removed by the summation in Eq. (12). Note that we are updating M^{N_b+1} conditional estimates in Eq. (11), whereas only M^{N_b} "unconditional" estimates are computed in Eq. (12). Each one of the "unconditional" estimates is then copied to the appropriate M subfilters whose subsequences differ only in symbol $d_j(k)$. The complete blind equalization algorithm is outlined in Table 1 and can be efficiently implemented using the parallel filter bank structure shown in Fig. 2.

The blind equalizer structure can be viewed as a bank of *conditional* channel estimators. Observe that there are $N=M^{N_b+1}$ single-input, single-output adaptive finite-impulse-response (FIR) filters comprised of the coefficient estimates $\hat{\mathbf{b}}_i(k-1)$, $i=1,\ldots,M^{N_b+1}$. The filter inputs are determined by all possible subsequence vectors $\{\mathbf{h}_i(k)\}$, and each filter output $\hat{r}_i(k)$ is generated according to the inner product in Eq. (9). Thus, the output of the i'th FIR filter corresponds to an estimate of the current received symbol $r(k)$, assuming that the i'th subsequence was transmitted (i.e., conditioned on the i'th subsequence). The filter outputs are then compared to the received sample $r(k)$ to generate a set of innovations or prediction error signals:

$$e_i(k)=r(k)-\hat{r}_i(k) \ , \tag{14}$$

which are used in the conditional measurement updates in Table 1.

The symbol decisions are determined from the MAP probability metrics. The optimum decision on symbol $d(k-N_b)$ is performed by computing the following marginal probability over all possible symbol values for $d(k-N_b)$:

$$\hat{d}(k-N_b)=\arg\max_{d(k-N_b)}\sum_{\{j:d_j(k-N_b)=d(k-N_b)\}}p(d_j^{k,N_b}|r^k) \ . \tag{15}$$

This MAP decision rule combined with the Bayesian update formulas are similar to those used in Ref. 12, except there they assumed that the channel was known *a priori*. The work in Ref. 12 did not consider the problem of channel estimation; thus, the likelihood computations are simpler than those required of the algorithm in this paper.

In practice, we have found that only one of the metrics, $p(d_i^{k,N_b}|r^k)$, converges to 1, while all others approach 0. As a result, only one term contributes substantially to the summation in Eq. (15). A suboptimal decision rule first determines the subsequence associated with the largest metric, i.e.,

$$\hat{d}_i^{k,N_b}=\arg\max_{d_i^{k,N_b}}p(d_i^{k,N_b}|r^k) \ , \tag{16}$$

and the symbol is then chosen according to

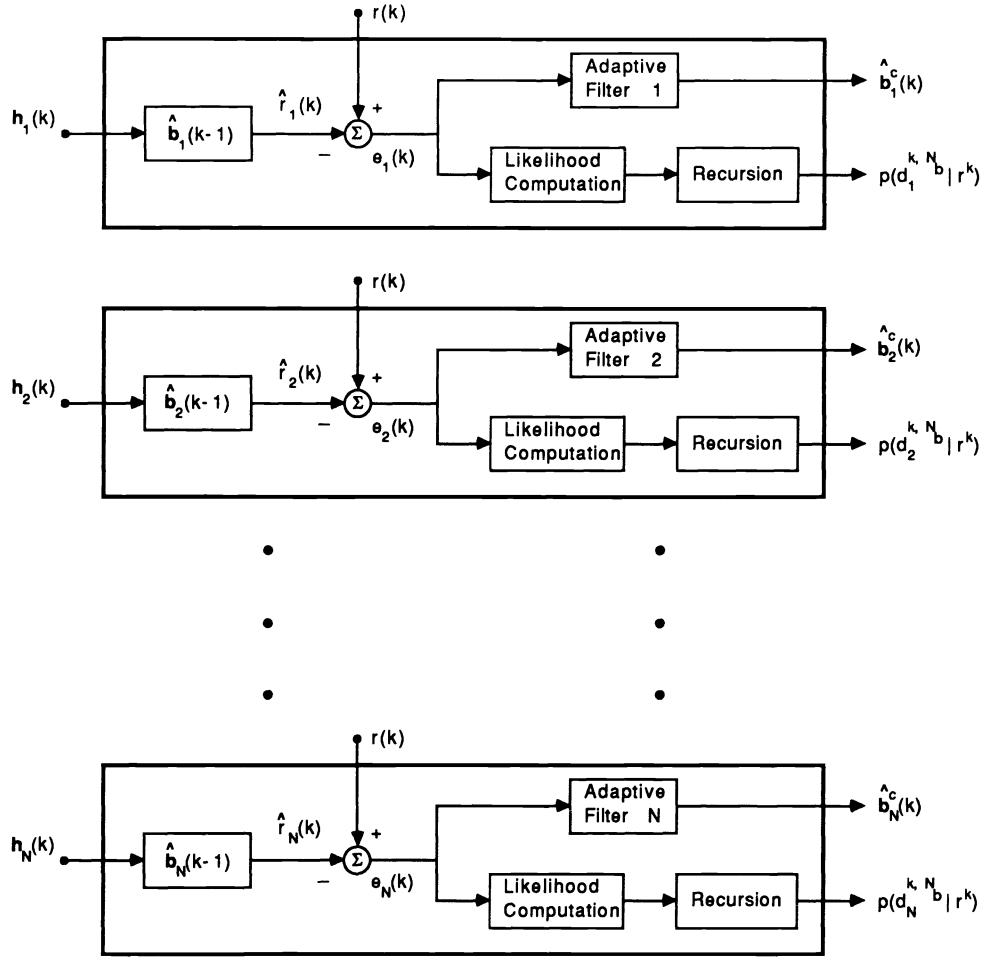

Fig. 2 Blind equalizer using parallel LMS adaptive filters.

Table 1 LMS Bayesian blind equalization algorithm.

Define Observation Vector

$$\mathbf{h}_i(k) = [d_i(k), \ldots, d_i(k - N_b)]$$

Compute Signal Estimates

$$\hat{r}_i(k) = \mathbf{h}_i(k)\hat{\mathbf{b}}_i(k - 1)$$

Compute Measurement Innovations

$$\epsilon_i(k) = r(k) - \hat{r}_i(k)$$

Compute Conditional Channel Estimates

$$\hat{\mathbf{b}}_i^c(k) = \hat{\mathbf{b}}_i(k - 1) + \mu(k)\mathbf{h}_i^H(k)\epsilon_i(k)$$

Update Probability Metrics

$$p(d_i^{k,N_b}|r^k) = \frac{1}{c}\mathcal{N}\left[r(k); \hat{r}_i(k), \sigma^2\right] \sum_{\{j:d_j^{k-1,N_b} \in d_i^{k,N_b}\}} p(d_j^{k-1,N_b}|r^{k-1})$$

Compute Unconditional Channel Estimates

$$\hat{\mathbf{b}}_i(k) = \sum_{\{j:d_j^{k,N_b} \in d_i^{k+1,N_b}\}} \hat{\mathbf{b}}_j^c(k) \frac{p(d_j^{k,N_b}|r^k)}{\sum_{\{m:d_m^{k,N_b} \in d_i^{k+1,N_b}\}} p(d_m^{k,N_b}|r^k)}$$

$$\hat{d}(k-N_b) = \hat{d}_i(k-N_b) \quad . \tag{17}$$

Note that the suboptimal rule in Eq. (16) provides us with a decision on the *entire* subsequence $\hat{d}_i^{k,N_b}$ corresponding to the largest metric. This implies that we could have made a decision at time k on any of the N_b+1 symbols in $\hat{d}_i^{k,N_b}$, whereas in Eq. (17) a decision is made only on symbol $d(k-N_b)$. We shall see how this particular choice allows us to cascade a decision-feedback filter with the MAP estimator, thereby reducing its complexity.

One possible drawback to the Bayesian algorithm is that M^{N_b+1} measurement updates must be computed at each iteration. To alleviate this complexity problem, a simplified algorithm using RSSE was considered.[14] In this method, the M^{N_b+1} subsequences are grouped into $J \leq M^{N_b+1}$ reduced-state sequences according to the Ungerboek set partitioning principles.[19,20] The trade-off between the level of performance and the computational complexity is controlled by the particular choice for J. RSSE introduces an inherent decision feedback while computing the branch metrics. It has been reported[19] that for maximum-likelihood sequence

estimation, the degradation caused by this decision feedback is gradual as one reduces J from that of the full algorithm ($J=M^{N_b+1}$) to that of the standard DFE ($J=1$).

The symbol-by-symbol MAP sequence estimation algorithm in Ref. 12 is basically equivalent to MLSE since the channel is known *a priori*. Hence, the performance/complexity trade-off one would expect with RSSE applied to the MAP algorithm is similar to the results reported for the MLSE-based Viterbi algorithm (VA). However, when the channel is unknown *a priori* and is being estimated adaptively, the degradation in performance introduced by RSSE can be unacceptably high. This was reported in our previous work,[14] where we concluded that RSSE may not be a suitable method for reducing the complexity of the *blind* MAP estimator.

Various *preprocessing* techniques designed to reduce the complexity of the Viterbi algorithm (for MLSE) by effectively reducing the channel memory are not directly viable for blind adaptation. Truncating the channel impulse response to a specified length and shape (for which the Viterbi decoder is designed) using a linear equalizer[21,22] or a DFE[23] requires off-line (batch) or on-line (training-based) estimation of the preprocessor coefficients. Furthermore, the DFE approach[23] operates independently of the VA and does not utilize the more reliable postdecoder decisions of the VA.

A method of combining a predictive DFE with the VA was recently introduced,[24] where a periodic interleaver/deinterleaver pair is used to generate the same delay as in the VA, enabling postdecoding decisions to be used by the noise predictor. However, this approach[24] and the improvement proposed in Ref. 25 suffer from a long throughput delay, which may be unacceptable for some telecommunications applications.

In contrast to the Viterbi algorithm, the symbol-by-symbol MAP algorithm of Abend and Fritchman[12] produces *delay-free* decisions. These reliable, postdecoding decisions can then be filtered by a decision-feedback *postprocessor*, thereby effectively truncating the channel memory seen by the MAP detector. Moreover, this postprocessor, like the MAP filter bank, can be adapted blindly using a simple gradient algorithm, as shown in Sec. 3.

3 Bayesian/DF Algorithm (BDFA)

Consider a linear transversal channel with an impulse response spanning N_b+1+N_a symbol intervals. Denoting the first N_b+1 channel coefficients by $\{b_m(k)\}$, $m=0,1,\ldots,N_b$, and the remaining N_a coefficients by $\{a_m(k)\}$, $m=1,2,\ldots,N_a$, the received signal $r(k)$ can be expressed as

$$r(k)=\sum_{m=0}^{N_b} b_m(k)d(k-m) + \sum_{m=1}^{N_a} a_m(k)d(k-N_b-m)+n(k) \ , \tag{18}$$

where $n(k)$ is a zero-mean, complex white Gaussian noise process with variance σ_n^2. By partitioning the channel coefficients in this way, we assume that $\{b_m(k)\}$ are the dominant coefficients, e.g.,

$$|b_i(k)| \geq |a_j(k)|, \quad \forall i\in\{0,\ldots,N_b\}, \ \forall j\in\{1,\ldots,N_a\}, \text{ and } \forall k \ . \tag{19}$$

This condition may not always be an accurate representation of most channels, but we use it here in our development of the BDFA for combined channel and sequence estimation. This assumption is further discussed in Sec. 5, where we summarize the properties of the BDFA.

Observe that Eq. (19) specifies that most of the energy in $r(k)$ is contributed by the $\{b_m(k)\}$ coefficients. To significantly minimize the measurement innovations, the MAP estimator should focus on these coefficients. Therefore, we could construct a MAP estimator assuming an *effective* channel memory of only N_b+1 symbol intervals. The computational savings from storing only M^{N_b+1} states (compared to the original $M^{N_b+1+N_a}$ states) can be considerable, especially for $N_a >> N_b$ and $M>2$. Moreover, under the assumption in Eq. (19), we intuitively expect that

$$p[r(k)|d_i^{k,N_b},r^{k-1}] \approx p[r(k)|d_j^{k,N_b+N_a},r^{k-1}],\forall j: d_j^{k,N_b}=d_i^{k,N_b} \ , \tag{20}$$

indicating that the likelihoods are determined primarily by the most recent N_b+1 symbols: $\{d_i(k),d_i(k-1),\ldots,d_i(k-Nb)\}$. From Eq. (7), one would then expect the evolution of the MAP sequence probabilities to be influenced mainly by these N_b+1 symbols. Thus, the MAP estimator with only M^{N_b+1} states should work satisfactorily as a sequence estimator, with a performance bounded above by the full estimator of $M^{N_b+1+N_a}$ states. The performance degradation due to this "undermodeling" is directly related to the uncanceled ISI contributed by the symbols weighted by the $\{a_m(k)\}$ coefficients.

A simple, low-complexity way to remove the remaining ISI and estimate the entire channel impulse response is suggested by Fig. 3. A MAP estimator with M^{N_b+1} parallel LMS adaptive filters (similar to the bank structure in Fig. 2) is shown cascaded with a feedback filter of length N_a. The operation of the equalizer in Fig. 3 can be explained as follows. At time k, the feedback filter contains the previous MAP decisions $\{\hat{d}(k-N_b-1),\ldots,\hat{d}(k-N_b-N_a)\}$. The ISI contribution due to these symbols is removed by subtracting the output of the feedback filter from $r(k)$, yielding

$$s(k)=r(k)-\hat{\mathbf{d}}_f(k)\hat{\mathbf{a}}(k-1) \ , \tag{21}$$

where $\hat{\mathbf{a}}(k-1)$ is the feedback coefficient (column) vector given by

$$\hat{\mathbf{a}}(k-1)=[\hat{a}_1(k-1),\ldots,\hat{a}_{N_a}(k-1)]^T \ , \tag{22}$$

and $\hat{\mathbf{d}}_f(k)$ is the corresponding signal (row) vector containing the previous MAP decisions:

$$\hat{\mathbf{d}}_f(k)=[\hat{d}(k-N_b-1),\ldots,\hat{d}(k-N_b-N_a)] \ . \tag{23}$$

The LMS filter bank computes the estimates $\{\hat{s}_i(k)\}$ of $s(k)$, and generates the M^{N_b+1} innovations. These are used to update the subfilters and probability metrics in exactly the same way as the algorithm in Sec. 2 [except that here $s(k)$ and $\{\hat{s}_i(k)\}$ are used instead of $r(k)$ and $\{\hat{r}_i(k)\}$, respectively].

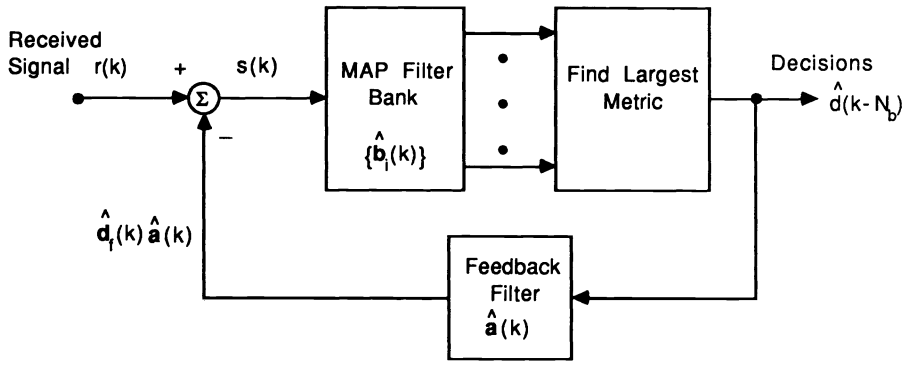

Fig. 3 Bayesian/DF blind adaptive equalizer.

The MAP estimator makes a decision on subsequence d_i^{k,N_b} using the same decision rule as in Eq. (16), which provides a decision on the entire subsequence of length N_b+1. We then choose symbol $d(k-N_b)$ according to Eq. (17), and this becomes the current input of the decision-feedback filter.

The coefficients $\hat{\mathbf{a}}(k-1)$ of the feedback filter are adjusted using the following gradient-descent algorithm:

$$\hat{\mathbf{a}}(k)=\hat{\mathbf{a}}(k-1)+\eta(k)\hat{\mathbf{d}}_f^H(k)e_f(k)\ , \tag{24}$$

where $\eta(k)$ is a scalar gain parameter and $e_f(k)$ is the innovations corresponding to that subsequence (among the M^{N_b+1} subsequences of the MAP estimator) which has the *largest* MAP metric in Eq. (7) at time k. The innovation residual $e_f(k)$ is given by

$$e_f(k)=s(k)-\hat{s}_f(k)\ , \tag{25}$$

where $\hat{s}_f(k)$ is the estimate $\hat{s}_i(k)$ with the largest MAP metric. Substituting $\hat{s}_f(k)$ and Eq. (21), yields

$$e_f(k)=[r(k)-\hat{\mathbf{d}}_f(k)\hat{\mathbf{a}}(k-1)]-\mathbf{h}_f(k)\hat{\mathbf{b}}_f(k-1)\ , \tag{26}$$

where the subfilter and subsequence corresponding to the largest MAP metric are denoted by $\hat{\mathbf{b}}_f(k-1)$ and $\mathbf{h}_f(k)$, respectively. The instantaneous gradient of $e_f^2(k)$ with respect to the feedback filter $\hat{\mathbf{a}}(k-1)$ [i.e., assuming that $\hat{\mathbf{b}}_f(k-1)$ is fixed] results in the LMS update in Eq. (24). Comparing Eq. (24) with Eq. (11), we see that the updates differ primarily by the choice of the scalar gains. Our experience suggests that choosing the DF filter gain $\eta(k)$ to be less than the gain $\mu(k)$ of the LMS adaptive filters in the MAP estimator is necessary for good performance. Apparently, the DF filter must adapt more slowly than the subfilters of the Bayesian estimator.

The complete BDFA is summarized in Table 2. Comparing it with Table 1, observe that this lower complexity algorithm involves only an extra update equation corresponding to the feedback filter. There is also an extra adder at the input of the MAP estimator to subtract from $r(k)$ the estimate of the ISI contributed by the channel coefficients $\{a_m(k)\}$.

Table 2 Bayesian/DF algorithm (BDFA).

Define Observation Vector
$$\mathbf{h}_i(k)=[d_i(k),\ldots,d_i(k-N_b)]$$

Define Decision-Feedback Vector
$$\hat{\mathbf{d}}_f(k)=\left[\hat{d}(k-N_b-1),\ldots,\hat{d}(k-N_b-N_a)\right]$$

Subtract DF Output from Received Signal
$$s(k)=r(k)-\hat{\mathbf{d}}_f(k)\hat{\mathbf{a}}(k-1)$$

Compute Signal Estimates
$$\hat{s}_i(k)=\mathbf{h}_i(k)\hat{\mathbf{b}}_i(k-1)$$

Compute Measurement Innovations
$$e_i(k)=s(k)-\hat{s}_i(k)$$

Compute Conditional Channel Estimates
$$\hat{\mathbf{b}}_i^c(k)=\hat{\mathbf{b}}_i(k-1)+\mu(k)\mathbf{h}_i^H(k)e_i(k)$$

Update Probability Metrics
$$p(d_i^{k,N_b}|r^k)=\frac{1}{c}\mathcal{N}\left[s(k);\hat{s}_i(k),\sigma^2\right]\sum_{\{j:d_j^{k-1,N_b}\in d_i^{k,N_b}\}}p(d_j^{k-1,N_b}|r^{k-1})$$

Find Maximum Metric and Determine $\hat{d}(k-N_b),e_f(k)$

Update Feedback Coefficients
$$\hat{\mathbf{a}}(k)=\hat{\mathbf{a}}(k-1)+\eta(k)\hat{\mathbf{d}}_f^H(k)\epsilon_f(k)$$

Compute Unconditional Channel Estimates
$$\hat{\mathbf{b}}_i(k)=\sum_{\{j:d_j^{k,N_b}\in d_i^{k+1,N_b}\}}\hat{\mathbf{b}}_j^c(k)\frac{p(d_j^{k,N_b}|r^k)}{\sum_{\{m:d_m^{k,N_b}\in d_i^{k+1,N_b}\}}p(d_m^{k,N_b}|r^k)}$$

4 Computer Simulations

We now present several computer simulations of the BDFA. The FIR channel had seven complex coefficients with the following transfer function:

$$\begin{aligned}B(z)=&\,0.444487+(-0.0488658-j0.776700)z^{-1}\\&+(-0.440101+j0.0555976)z^{-2}\\&+(0.14+j0.15)z^{-3}+(0.20+j0.15)z^{-4}\\&+(0.04+j0.10)z^{-5}+0.05z^{-6}\ .\end{aligned} \tag{27}$$

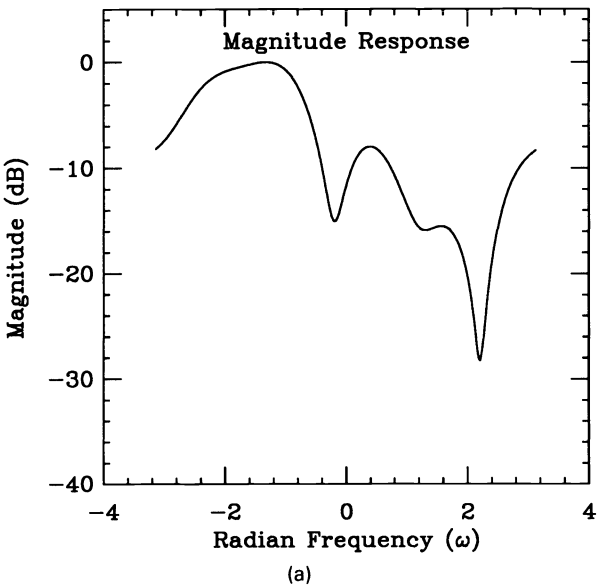

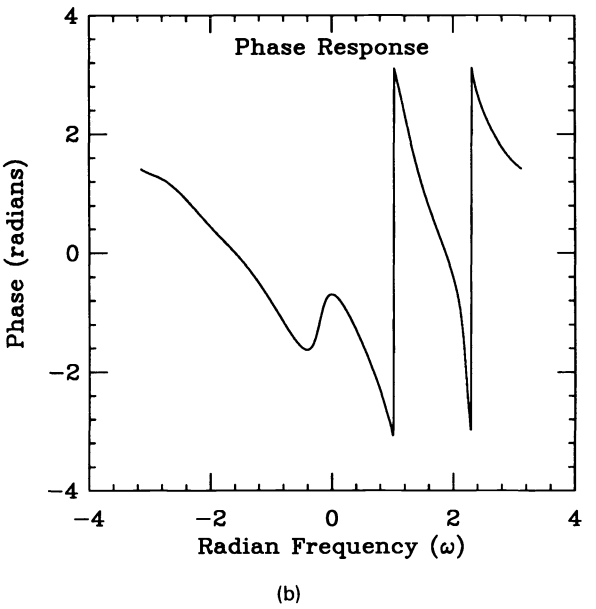

Fig. 4 Channel frequency response $B(\omega)$: (a) magnitude response and (b) phase response.

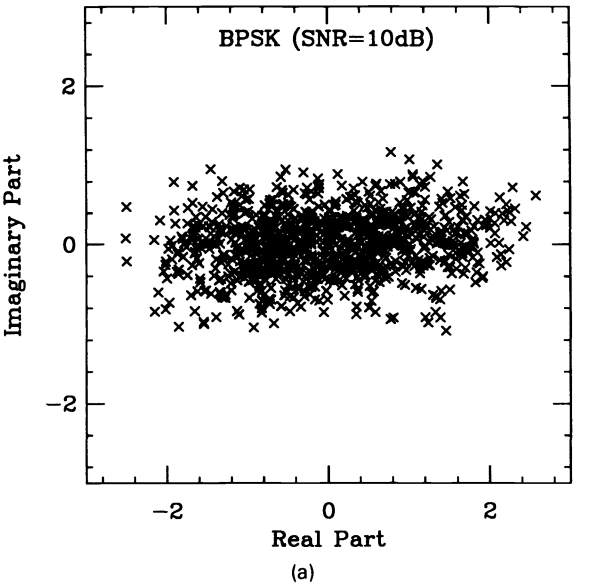

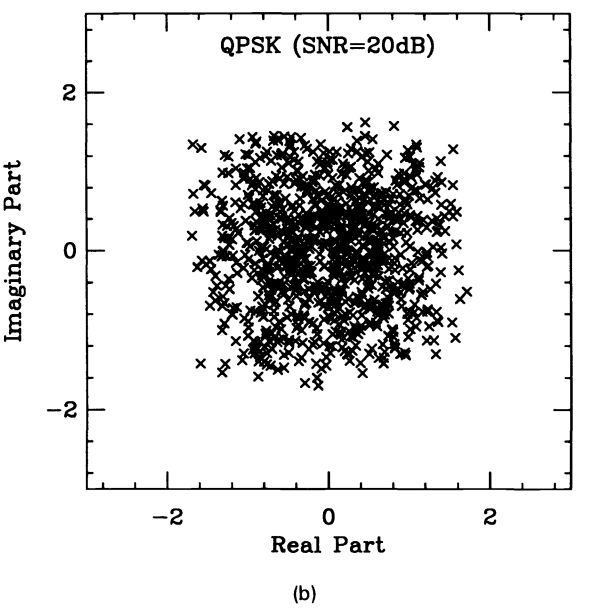

Fig. 5 Eye patterns before equalization: (a) BPSK (SNR = 10 dB) and (b) QPSK (SNR = 20 dB).

From the frequency response in Fig. 4, observe that this channel has inband nulls, which are very difficult to equalize with a transversal filter (as is the case with Bussgang-type blind algorithms). The eye patterns produced by this channel are shown in Fig. 5 for BPSK and quadrature phase-shift keying (QPSK) with SNR = 10 dB and SNR = 20 dB, respectively. Observe that in both cases the eye is closed prior to equalization. During demodulation, BPSK signals can be detected from either the in-phase or quadrature channel outputs alone. However, since we are also performing channel estimation, we have used a complex equalizer even for BPSK signaling. The SNR was defined in terms of the average symbol energy E_a and the noise power N_0 [i.e., $\text{SNR} = 10\log(E_a/N_0)$]. For convenience, energy-normalized signal constellations were chosen such that $E_a = 1$. In addition, the bit interval was set equal to one. Thus, for BPSK the transmitted symbol alphabet was ± 1, while for QPSK it was $\{\pm 1/(2)^{1/2}, \pm i/(2)^{1/2}\}$. The noise power N_0 was varied over a range of values in the simulations, and the probability metric variance σ^2 was fixed at 0.01 for all computer runs.

Since the channel is time-invariant, the algorithm was optimized to operate on stationary data. To reduce the misadjustment error at steady state, the step sizes $\mu(k)$ (MAP section) and $\eta(k)$ (DF section) were chosen to decay at the rate β (i.e., $\mu(k) = \beta^k \mu_0$ and $\eta(k) = \beta^k \eta_0$). For BPSK, we used $\beta = 0.99$, $\mu_0 = 0.5$, and $\eta_0 = 0.1$, while for QPSK, $\beta = 0.999$, $\mu_0 = 0.15$, and $\eta_0 = 0.03$. All M^{N_b+1} coefficients in the MAP filter bank were initialized to the same value, i.e., $\hat{b}_{i,m}(0) = c$, such that $\Sigma_{m=0}^{N_b} |\hat{b}_{i,m}(0)|^2 = (N_b + 1)|c|^2 = 1$. The coefficients and delay-line signals of the DF filter were all initialized to zero. This initialization and the choice of different gains for the MAP filter bank and the DF filter

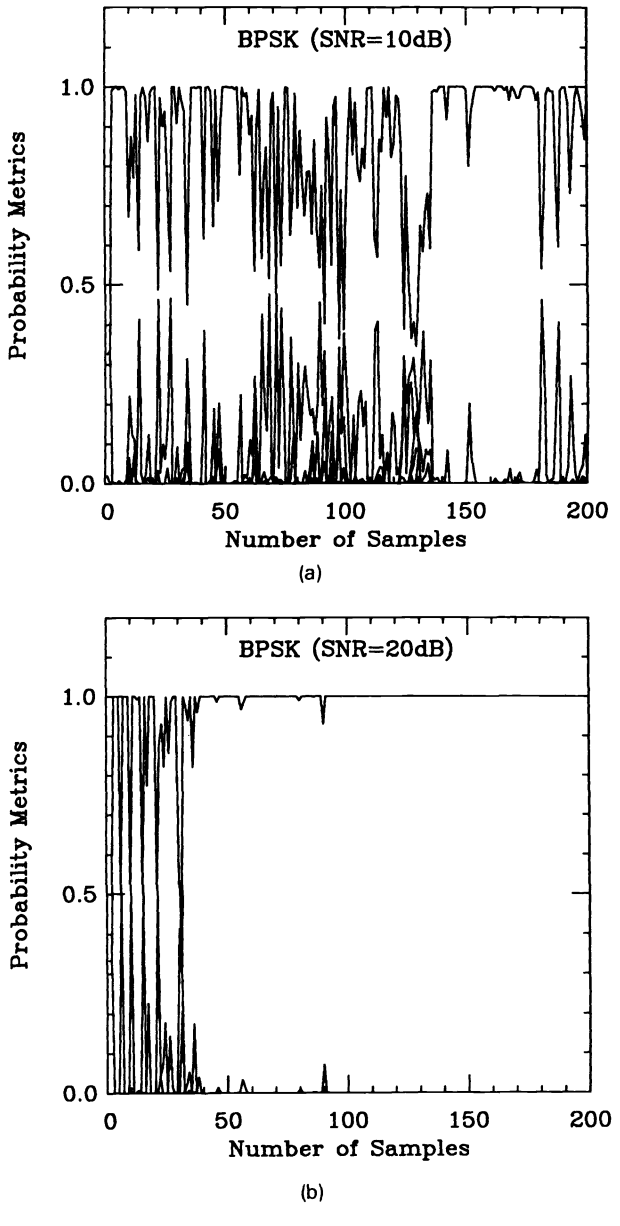

Fig. 6 Evolution of the probability metrics (BPSK): (a) SNR = 10 dB and (b) SNR = 20 dB.

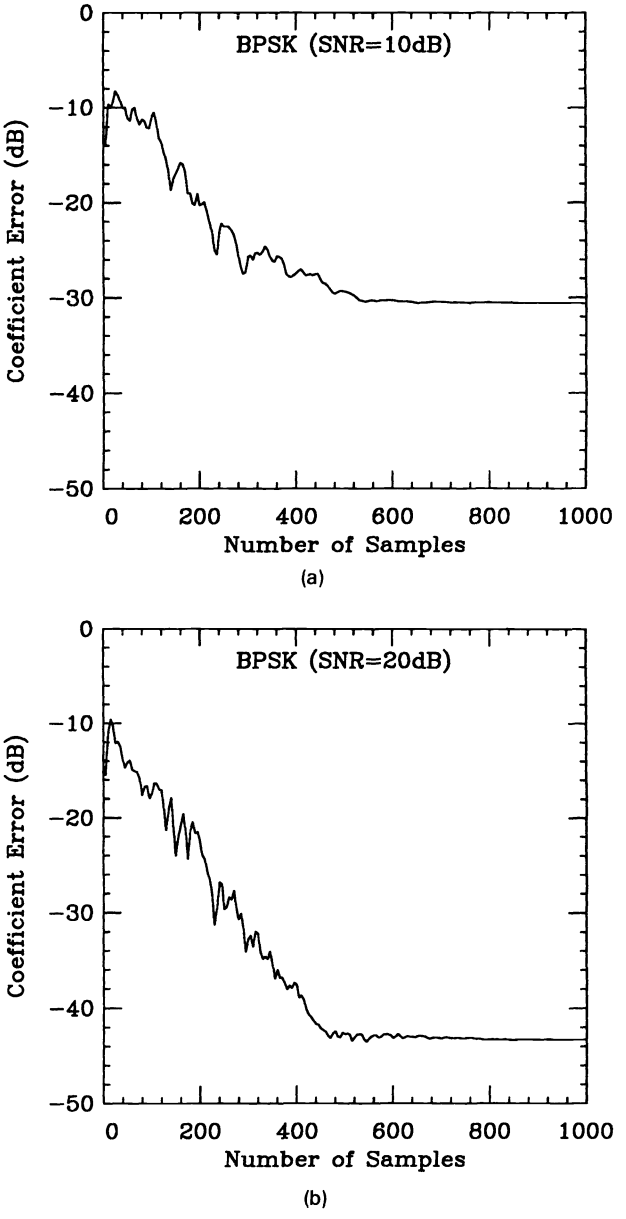

Fig. 7 Coefficient error trajectories (BPSK): (a) SNR = 10 dB and (b) SNR = 20 dB.

were done to mitigate the degradation due to error propagation during the initial iterations of the algorithm. In the following plots, only one computer run is shown for the probability metrics, whereas the coefficient error trajectories were averaged over 10 independent runs. In addition, the coefficient error curves were smoothed by a 10-weight moving-average filter.

Figures 6 to 9 illustrate the convergence properties of the BDFA. The MAP estimator had M^3 states and the DF filter had four coefficients; this choice was motivated by the fact that the channel impulse response has most of its energy in the first three weights (thus, $N_b+1=3$). Figure 6 shows the evolution of the equalizer probability metrics [i.e., the quantities in Eq. (7)] for BPSK signaling and SNRs of 10 dB and 20 dB. Since the MAP subfilters each have three coefficients and $M=2$, there are eight possible subsequences and eight probability metrics. Observe that for the higher SNR, one of the metrics converges to 1 in less than 100 iterations. Although the metric trajectories are noisier for the lower SNR, there is still only one metric that dominates after convergence. Figure 7 shows the trajectories for the corresponding coefficient errors, which were obtained by averaging the squared error between the actual channel coefficients and those of the channel estimator with the *largest* probability metric, i.e.,

$$E(k)=\frac{1}{N_b+1+N_a}\left[\sum_{m=0}^{N_b}|\hat{b}_{f,m}(k-1)-b_m|^2+\sum_{m=1}^{N_a}|\hat{a}_m(k-1)-a_m|^2\right], \tag{28}$$

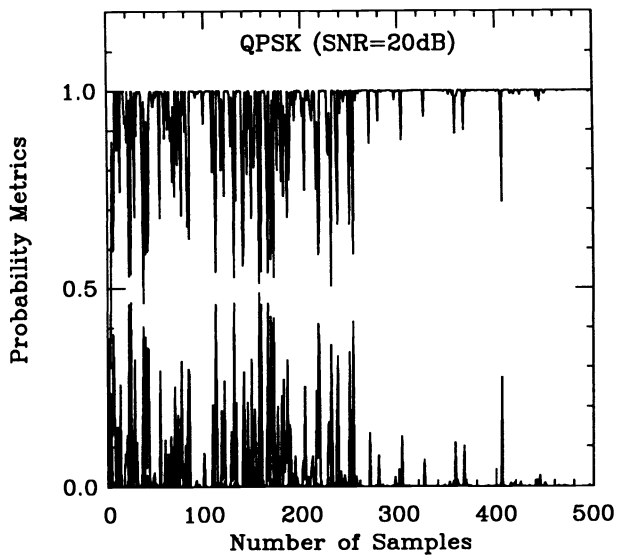

(a)

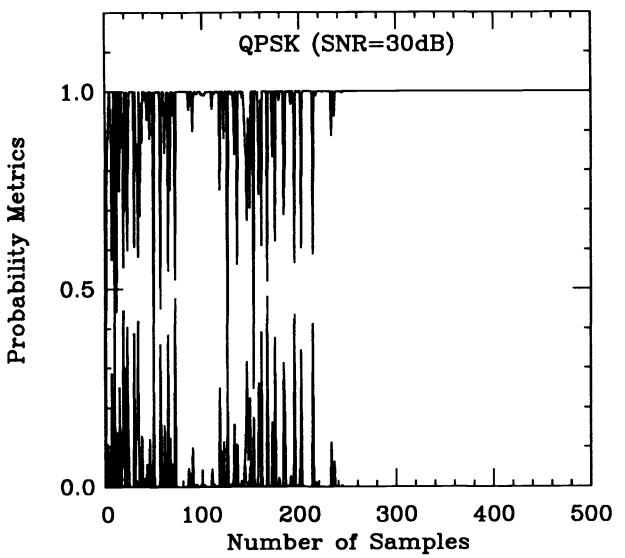

(b)

Fig. 8 Evolution of the probability metrics (QPSK): (a) SNR = 20 dB and (b) SNR = 30 dB.

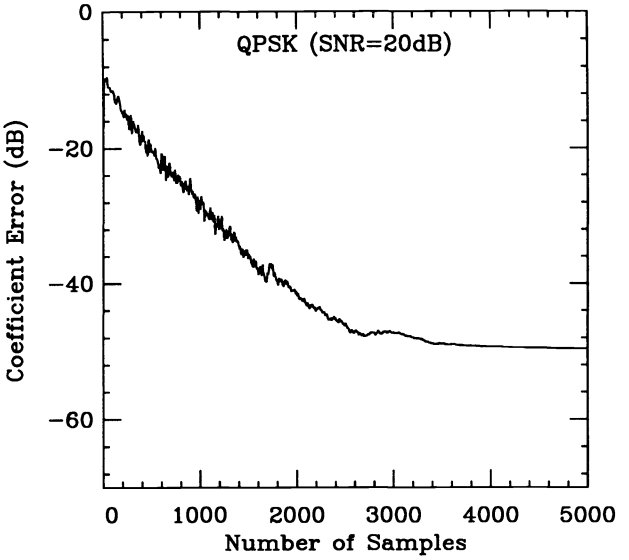

(a)

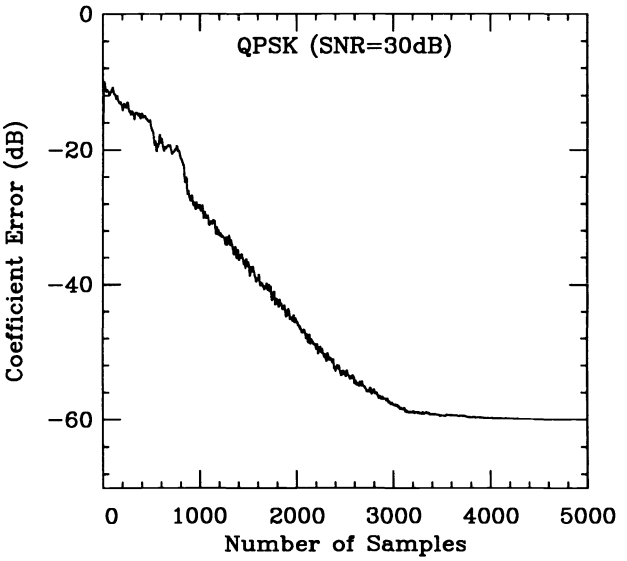

(b)

Fig. 9 Coefficient error trajectories (QPSK): (a) SNR = 20 dB and (b) SNR = 30 dB.

which also includes the coefficient error of the feedback filter. Observe that for SNR = 20 dB, this error is less than −40 dB by about 500 samples. By using a Kalman MAP algorithm, this convergence can be made much faster, e.g., within 100 samples (see the simulations in Ref. 14).

Figures 8 and 9 show the corresponding results for QPSK signaling and SNRs of 20 dB and 30 dB. In this case, since $M = 4$, there are 64 possible subsequences of which we plot only the eight largest metrics. Observe again that only one metric dominates after convergence, and that the metric trajectories are noisier for the lower SNR. In particular, for SNR = 30 dB, the BDFA metrics converge by 250 samples, while the coefficient error takes about 3500 samples to reach steady state.

The bit error rate (BER) was also computed for BPSK and QPSK signaling. Compensation was included for the group delay of the channel, and the BER was measured after reaching steady state, i.e., we discarded the initial 500 samples before counting symbol errors. The standard deviation of the BER estimation error was kept to within 5% by repeating the experiment a sufficient number of times.

For BPSK signaling, Fig. 10(a) shows the BER performance of the BDFA compared with that of the undermodeled MAP estimator (i.e., without a DF filter). Observe that the uncanceled ISI in the undermodeled 2^3-state MAP estimator causes a significant degradation in the steady-state performance. We have also included a performance curve for the optimal MAP estimator (with *a priori* known channel) of Abend and Fritchman.[12] In our earlier paper,[14] we had reported computer simulation results (on a different channel) showing that the full MAP estimator, using both the Kalman and LMS filters, achieves nearly the same performance as

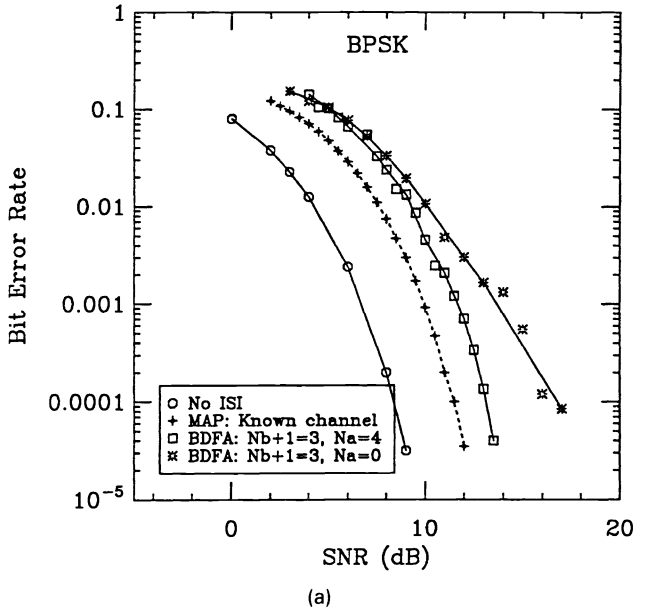

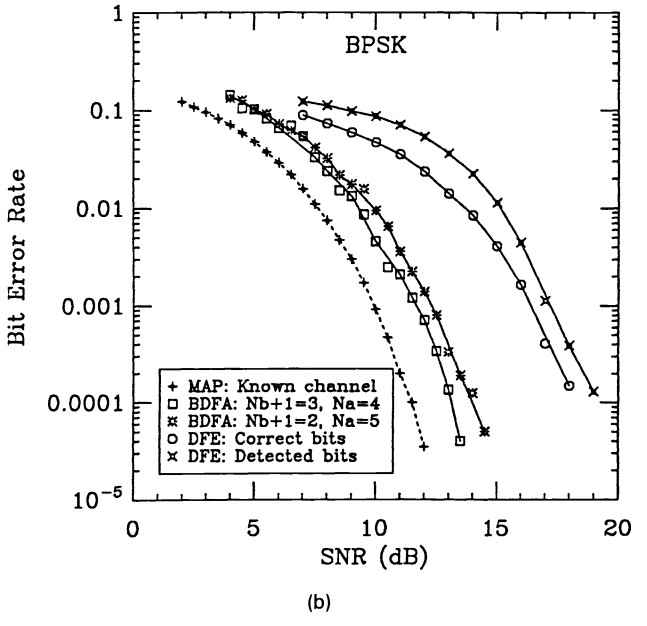

Fig. 10 BER performance curves (BPSK): (a) comparison with zero ISI case and (b) comparison with DFE.

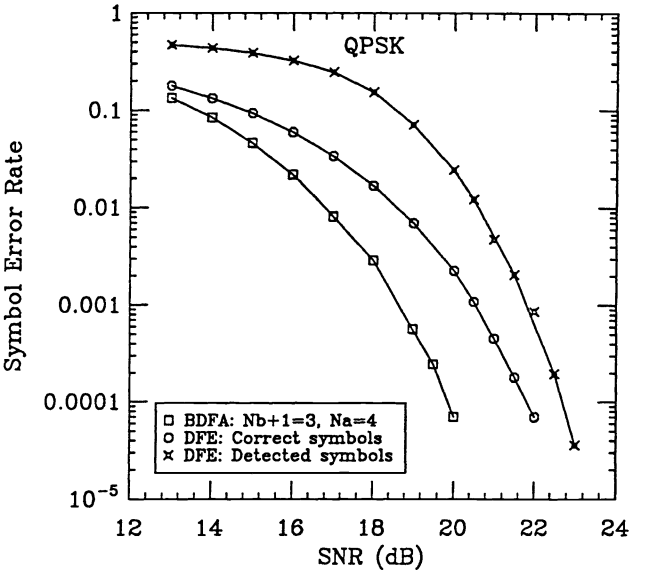

Fig. 11 SER performance curves (QPSK).

the algorithm in Ref. 12. Hence, this curve also represents the performance of the full 2^7-state blind MAP algorithm. Finally, for comparison purposes, the curve corresponding to zero ISI is also shown, which was analytically evaluated using the error function. In summary, we see that the BDFA has a loss in SNR of about 2 dB compared to the optimal MAP algorithm, but is superior to the undermodeled 2^3-state MAP estimator by about 3 dB (for a BER $\approx 10^{-3}$).

Figure 10(b) compares the BDFA to a seven-coefficient DFE for BPSK signals. Observe that the performance of the BDFA lies between that of the optimal MAP estimator and the DFE. The performance of the DFE for the channel in Eq. (27) was simulated with feedback of the correct symbols, and with feedback of the detected symbols. In particular, observe that the BDFA with just a four-state MAP detector, i.e., $N_b+1=2$ and $N_a=5$, has a performance about 4 dB better than that of the DFE using detected symbols. This result illustrates that the order of the MAP section need not exactly match the number of dominant channel coefficients to achieve good performance.

Figure 11 compares the BDFA with a seven-coefficient DFE for QPSK signaling. We have not evaluated the optimal MAP bound here, since it involves simulating the Abend and Fritchman algorithm over $4^7=16{,}384$ states! The BDFA used in the simulations has only $4^3=64$ channels in the MAP section, and a four-coefficient DF filter in cascade. Observe that the BDFA has a symbol error rate (SER) performance about 3 dB better than that of the DFE with detected symbols.

Finally, the BDFA was also tested for 16 quadrature amplitude modulation (QAM). Here again, the signal constellation was energy normalized by choosing the intersymbol spacing to be $2(16/160)^{1/2}=0.6324$. A six-coefficient channel with the following transfer function was used:

$$C(z)=(0.51+j0.32)+(0.47+j0.18)z^{-1}+(0.14+j0.15)z^{-2}+(0.20+j0.15)z^{-3}+(0.04+j0.10)z^{-4}+0.05z^{-5}\ , \tag{29}$$

which has the frequency response shown in Fig. 12. The eye pattern before equalization is shown in Fig. 13. This channel has only two dominant coefficients, so that the MAP section has $16^2=256$ states; the DF section thus has four coefficients. The algorithm parameters were $\beta=0.998$, $\mu_0=0.5$, and $\eta_0=0.1$, with an SNR = 35 dB. Figure 14 shows a trajectory of the *maximum* metric (of the 256 metrics) and the averaged coefficient error. Observe that this error is reduced below -30 dB in less than 3000 samples, illustrating that the algorithm performs well even for high-order signal constellations.

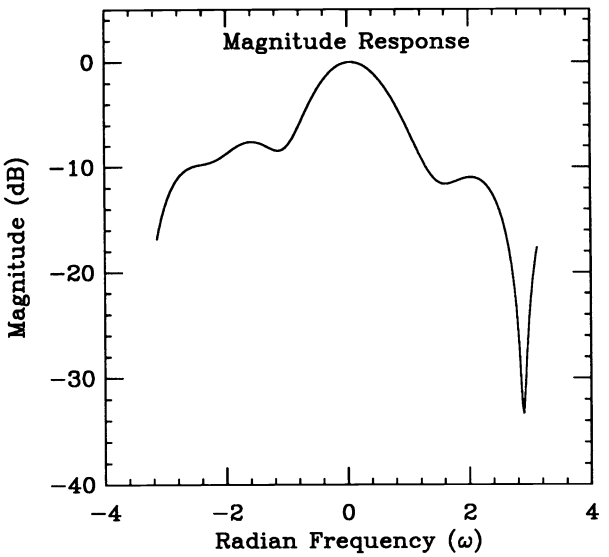

(a)

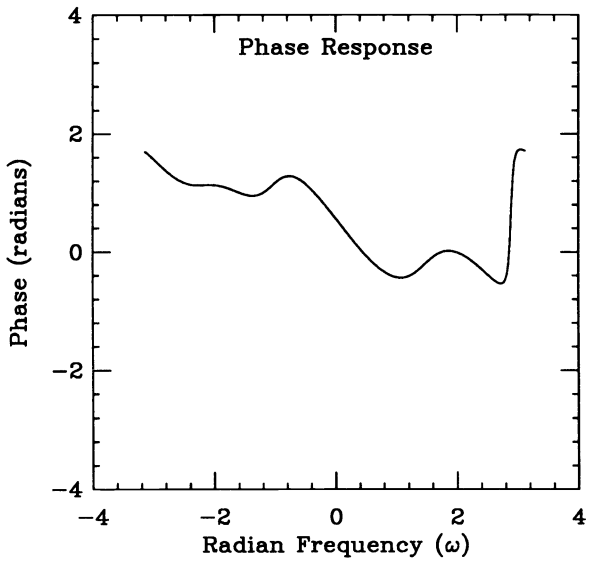

(b)

Fig. 12 Channel frequency response $C(\omega)$: (a) magnitude response and (b) phase response.

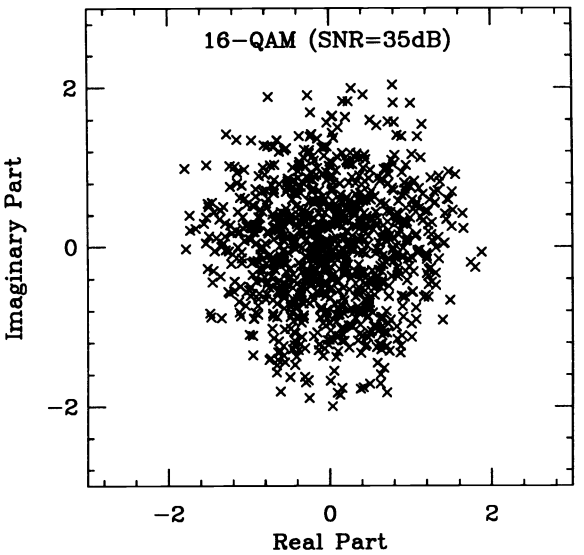

Fig. 13 16-QAM eye pattern before equalization.

5 Discussion

In this section, we describe some properties of the Bayesian/DF algorithm that are based largely on simulation studies. To understand the potential savings in complexity that is possible, consider the real channels shown in Fig. 15 with coefficients $\{b_m\}$, $m=0,1,\ldots,10$. In the first channel, observe that most of the received signal energy is contributed by coefficients $\{b_0,\ldots,b_3\}$. According to the model in Eq. (19), $N_b+1=4$ would be a reasonable choice. Hence, we require a MAP estimator with only M^4 states in cascade with a DF filter having seven coefficients. Simulations demonstrate that the coefficient estimate vector of the blind algorithm, $[\hat{\mathbf{b}}_i(k-1)^T\hat{\mathbf{a}}(k-1)^T]^T$, converges to the true channel estimates $[b_0,b_1,\ldots,b_{10}]^T$. In contrast, the full MAP sequence estimator would require M^{11} subfilters. For example, with $M=2$ (BPSK), the full MAP estimator would have 2048 filters, each of length 11, and these would be updated every time instant. The BDFA would require only 16 subfilters, each of length four, and a single feedback filter of length seven. Obviously, this is a considerable reduction in the computational complexity.

Consider the second real channel shown in Fig. 15, which does not satisfy the channel shape model in Eq. (19). Observe here that no choice of N_b (other than $N_b=10$, the total length of the given channel) satisfies the condition in Eq. (19). As a result, the BDFA will not, in general, provide us with a complete set of channel estimates. However, as a sequence estimator, the degradation in performance is minimal. The reason for this can be argued as follows. Suppose that we decide to limit the MAP complexity to M^4 states, and cascade a seven-weight DF section to handle the remaining coefficients. To minimize the residuals, the MAP estimator will generally converge to the dominant coefficients of the impulse response, i.e., $\{b_2,\ldots,b_5\}$. The "eye" is opened sufficiently so that the feedback decisions are reasonably accurate, and the DF filter converges to the tail coefficients $\{b_6,\ldots,b_{10}\}$. This implies that b_0 and b_1 are not estimated, and the ISI contributed by the symbols $d(k)$ and $d(k-1)$ is not canceled. As a result, the performance degradation in SNR will be directly determined by these uncanceled ISI terms. However, simulations over a wide variety of channels demonstrate that the loss in SNR incurred due to this undermodeling is small—typically <1 dB. For example, note in Fig. 10(b) that the BDFA with only a four-state MAP section has a performance within 1 dB of that obtained by using an eight-state MAP section.

Our simulation studies also indicate that it is preferable to choose different gain constants for the MAP filter bank and the DF filter. We have found that choosing $\eta(k)=\gamma\mu(k)$, with $0.20<\gamma<0.25$, usually provides good performance. By controlling the gain of the feedback filter, we can mit-

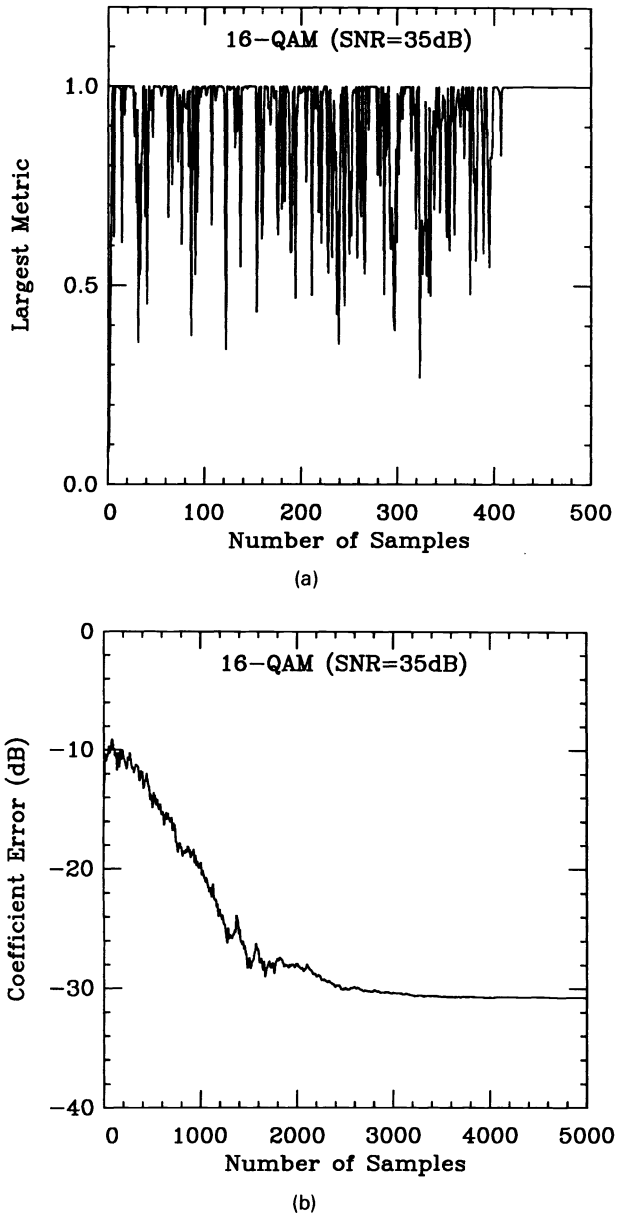

Fig. 14 16-QAM performance: (a) evolution of largest metric and (b) coefficient error trajectory.

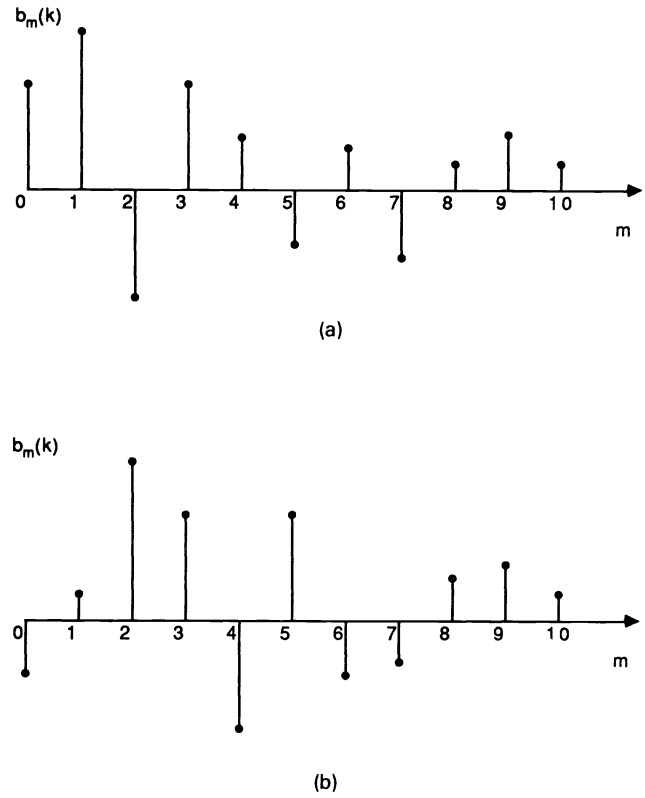

Fig. 15 (a) Channel satisfying the model in Eq. (19) and (b) channel violating the model in Eq. (19).

igate the effects of error propagation due to incorrect MAP decisions. This is especially important during the first few iterations when the MAP decisions are unreliable. Typically, the DF filter coefficients would be initialized to zero, and they would be adapted with a step size that is smaller than that used in the MAP section. Thus, the feedback coefficients initially remain near zero and have minimal influence on the received symbols. Once the MAP estimator becomes more reliable, the DF filter then automatically reduces the ISI further by removing the effects of the tail of the channel impulse response.

Note that this feature of having separate gains for the MAP and feedback sections is not possible with RSSE. Consequently, during the initial iterations of the RSSE-MAP estimator, the MAP metric computations may result in the wrong reduced-state sequence being selected to represent the particular subset. Using the incorrect representative state is equivalent to propagating the wrong decisions through the DF section. Also note that, in terms of complexity, the RSSE-MAP algorithm still needs to store $M^{N_b+1+N_a}$ subsequences, although it needs only M^{N_b+1} subfilters.

6 Conclusion

A new blind equalization algorithm has been presented that is a low-complexity approximation to the optimal MAP sequence estimator for *a priori* unknown channels. The channel estimates are derived from a bank of parallel LMS adaptive filters,[14,15] whose innovations are used to update a set of MAP (Bayesian) probability metrics. A decision-feedback mechanism is employed to effectively truncate the channel memory as seen by the MAP estimator. By controlling the complexity apportionment between the Bayesian and DF sections, the performance of the new algorithm varies between that of the optimal MAP algorithm and the standard DFE. Thus, there is a trade-off between the amount of computational complexity that can be afforded and the degree of robustness to catastrophic error propagation. The rapid convergence properties of this algorithm, even for channels with in-band nulls, makes it a suitable blind equalization technique for narrowband applications. Being a combined channel and sequence estimation scheme, the Bayesian/DF algorithm (like the blind MAP algorithms in Ref. 14)

may provide improved equalization performance compared to Bussgang-type blind algorithms, especially for channels with severe intersymbol interference.

Acknowledgments

This work was sponsored in part by the University of California MICRO program, Applied Signal Technology, Inc., and Sonatech, Inc.

References

1. S. Haykin, *Adaptive Filter Theory,* 2nd ed., Prentice-Hall, Englewood Cliffs, N.J. (1991).
2. Y. Sato, "A method of self-recovering equalization for multilevel amplitude-modulation systems," *IEEE Trans. Commun.* **COM-23,** 679–682 (June 1975).
3. D. N. Godard, "Self-recovering equalization and carrier tracking in two-dimensional data communication systems," *IEEE Trans. Commun.* **COM-28,** 1867–1875 (Nov. 1980).
4. J. R. Treichler and B. G. Agee, "A new approach to multipath correction of constant modulus signals," *IEEE Trans. Acoust. Speech Signal Process.* **ASSP-31,** 459–472 (April 1983).
5. A. Benveniste and M. Goursat, "Blind equalizers," *IEEE Trans. Commun.* **COM-32,** 871–883 (Aug. 1984).
6. G. Picchi and G. Prati, "Blind equalization and carrier recovery using a 'stop-and-go' decision-directed algorithm," *IEEE Trans. Commun.* **COM-35,** 877–887 (Sep. 1987).
7. S. Bellini, "Bussgang techniques for blind equalization," in *Proc. IEEE Global Telecommun. Conf.,* Houston, Tx., pp. 1634–1640 (Dec. 1986).
8. V. Weerackody and S. A. Kassam, "Blind adaptive equalization using dual-mode algorithms," in *Proc. Twenty-Fourth Asilomar Conf. on Signals, Systems, and Computers,* Pacific Grove, Calif., pp. 263–267 (Nov. 1990).
9. Z. Ding, C. R. Johnson, Jr., and R. A. Kennedy, "On the admissibility of blind adaptive equalizers," in *Proc. IEEE Int. Conf. on Acoustics, Speech, and Signal Processing,* Albuquerque, N.M., pp. 1707–1710 (April 1990).
10. J. J. Shynk, R. P. Gooch, K. Giridhar, and C. K. Chan, "A comparative performance study of several blind equalization algorithms," *Proc. SPIE* **1565,** 102–117 (July 1991).
11. R. Pan and C. L. Nikias, "The complex cepstrum of higher order cumulants and nonminimum phase system identification," *IEEE Trans. Acoust., Speech, Signal Process.* **36,** 186–205 (Feb. 1988).
12. K. Abend and B. D. Fritchman, "Statistical detection for communication channels with intersymbol interference," *IEEE* **58,** 779–785 (May 1970).
13. R. A. Iltis, "A Bayesian channel and timing estimation algorithm for use with MLSE," in *Proc. Twenty-Fourth Asilomar Conf. on Signals, Systems, and Computers,* Pacific Grove, Calif., pp. 119–123 (Nov. 1990).
14. R. A. Iltis, J. J. Shynk, and K. Giridhar, "Bayesian algorithms for blind equalization using parallel adaptive filtering," *IEEE Trans. Commun.* (submitted 1991).
15. R. A. Iltis, J. J. Shynk, and K. Giridhar, "Recursive Bayesian algorithms for blind equalization," in *Proc. Twenty-Fifth Asilomar Conf. on Signals, Systems, and Computers,* Pacific Grove, Calif., pp. 710–715 (Nov. 1991).
16. N. Seshadri, "Joint data and channel equalization using fast blind trellis search techniques," in *Proc. IEEE Global Telecommun. Conf.,* San Diego, Calif., pp. 1659–1663 (Dec. 1990).
17. M. Ghosh and C. L. Weber, "Maximum-likelihood blind equalization," *Proc. SPIE* **1565,** 188–195 (July 1991).
18. M. Feder and J. A. Catipovic, "Algorithms for joint channel estimation and data recovery—Application to equalization in underwater communications," *IEEE J. Oceanic Engin.* **16,** 42–55 (Jan. 1991).
19. M. V. Eyuboğlu and S. U. H. Qureshi, "Reduced-state sequence estimation with set partitioning and decision feedback," *IEEE Trans. Commun.* **36,** 13–20 (Jan. 1988).
20. G. Ungerboeck, "Channel coding with multilevel/phase signals," *IEEE Trans. Inform. Theory* **IT-28,** 55–67 (Jan. 1982).
21. S. U. H. Qureshi and E. E. Newhall, "An adaptive receiver for data transmission over time-dispersive channels," *IEEE Trans. Inform. Theory* **IT-19,** 448–457 (July 1973).
22. D. D. Falconer and F. R. Magee, Jr., "Adaptive channel memory truncation for maximum-likelihood sequence estimation," *Bell Sys. Tech. J.* **52,** 1541–1562 (Nov. 1973).
23. W. U. Lee and F. S. Hill, "A maximum-likelihood sequence estimator with decision-feedback equalization," *IEEE Trans. Commun.* **COM-25,** 971–979 (Sep. 1977).
24. M. V. Eyuboğlu, "Detection of coded modulation signals on linear, severely distorted channels using decision-feedback noise prediction with interleaving," *IEEE Trans. Commun.* **36,** 401–409 (April 1988).
25. K. Zhou, J. G. Proakis, and F. Ling, "Decision-feedback equalization of time-dispersive channels with coded modulation," *IEEE Trans. Commun.* **38,** 18–24 (Jan. 1990).

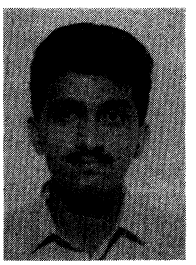

K. Giridhar received the BSc degree in applied sciences from the P.S.G. College of Technology, Coimbatore, India, and the ME degree in electrical communication engineering from the Indian Institute of Science, Bangalore, in 1985 and 1989, respectively. From June 1989 to March 1990, he worked with the Central Research Laboratory of Bharat Electronics, Ltd., Bangalore. Since April 1990, he has been a doctoral student in the Department of Electrical and Computer Engineering at the University of California, Santa Barbara. His research interests are in adaptive filtering, communication systems, neural networks for signal processing, and sensor array processing.

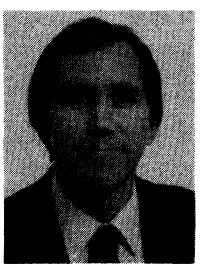

John J. Shynk received the BS degree in systems engineering from Boston University, Mass., in 1979, the MS degree in electrical engineering and in statistics, and the PhD degree in electrical engineering from Stanford University, Calif., in 1985, and 1987, respectively. From 1979 to 1982, he was a member of the technical staff in the Data Communications Performance Group at AT&T Bell Laboratories, Holmdel, N.J., where he formulated performance models for voiceband data communications. He was a research assistant from 1982 to 1986 in the Electrical Engineering Department at Stanford University, where he worked on frequency-domain implementations of adaptive IIR filter algorithms. Since 1987, he has been with the Department of Electrical and Computer Engineering at the University of California, Santa Barbara, where he is currently an assistant professor. His current research interests include developing and analyzing efficient adaptive signal processing algorithms for blind equalization and neural networks. He recently served as associate editor for adaptive filtering of the *IEEE Transactions on Signal Processing*. Shynk is a member of Tau Beta Pi, Sigma Xi, IEEE, and INNS.

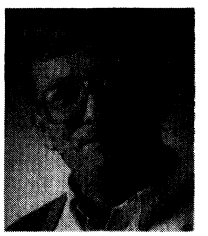

Ronald A. Iltis received the BA degree in biophysics from The Johns Hopkins University in 1978, the MSc in engineering from Brown University in 1980, and the PhD in electrical engineering from the University of California, San Diego, in 1984. Since 1984, he has been on the faculty of the Department of Electrical and Computer Engineering at the University of California, Santa Barbara, where he is currently an associate professor. Between 1980 and 1981, he was employed at General Dynamics in San Diego, and from 1982 to 1984 he was employed part-time at MA/COM Linkabit, where he developed software for vocoders and modems. His current research interests are in spread-spectrum communications, multisensor/multitarget tracking, and neural networks. Iltis was previously an editor for the *IEEE Transactions on Communications*. He is also recipient of the 1990 Fred W. Ellersick award for best paper at the IEEE MILCOM conference.